



2D characterization at submicron scale of crack propagation of 17-4PH parts produced by Atomic Diffusion Additive Manufacturing (ADAM) process

Claire Gong, Joseph Marae Djouda, Abdelhamid Hmima, Fabrice Gaslain, Mahdi Chemkhi, Thomas Maurer, Benoît Panicaud

► To cite this version:

Claire Gong, Joseph Marae Djouda, Abdelhamid Hmima, Fabrice Gaslain, Mahdi Chemkhi, et al.. 2D characterization at submicron scale of crack propagation of 17-4PH parts produced by Atomic Diffusion Additive Manufacturing (ADAM) process. Second European Conference on the Structural Integrity of Additively Manufactured Materials, Sep 2021, Virtuel, Norway. pp.13 - 19, 10.1016/j.prostr.2021.12.003 . hal-03864734

HAL Id: hal-03864734

<https://minesparis-psl.hal.science/hal-03864734>

Submitted on 16 Dec 2022

HAL is a multi-disciplinary open access archive for the deposit and dissemination of scientific research documents, whether they are published or not. The documents may come from teaching and research institutions in France or abroad, or from public or private research centers.

L'archive ouverte pluridisciplinaire **HAL**, est destinée au dépôt et à la diffusion de documents scientifiques de niveau recherche, publiés ou non, émanant des établissements d'enseignement et de recherche français ou étrangers, des laboratoires publics ou privés.

The second European Conference on the Structural Integrity of Additively Manufactured Materials

2D characterization at submicron scale of crack propagation of 17-4PH parts produced by Atomic Diffusion Additive Manufacturing (ADAM) process

Claire Gong^{a,*}, Joseph Marae Djouda^{b,c}, Abdelhamid Hmima^a, Fabrice Gaslain^d, Mahdi Chemkhi^{b,c}, Thomas Maurer^a, Benoît Panicaud^e

^aLight, Nanomaterials, Nanotechnologies, CNRS ERL 7004, University of Technology of Troyes, Troyes, France

^bEPF Graduate School of Engineering, 2 rue Fernand Sastre, 10430 Rosières-Près-Troyes, France

^cUniversité Paris-Saclay, ENS Paris-Saclay, CNRS, LMT – Laboratoire de Mécanique et Technologie, Gif-sur-Yvette, France

^dMINES ParisTech, PSL - Research University, Centre des Matériaux CNRS UMR 7633, BP 87 91003 Evry, France

^eLife Assessment of Structures, Materials, mechanics and Integrated Systems, University of Technology of Troyes, Troyes, France

Abstract

In this study, a Surface Mechanical Attrition Treatment (SMAT) is applied to a 17-4PH single edge notched tension (SENT) sample made by Atomic Diffusion Additive Manufacturing (ADAM). Grating of gold nanoparticles allowing multiscale characterizations is deposited on the surface of specimen by electron beam lithography. In-situ tensile test is carried out and images of the surface are recorded. The crack propagation is followed and the local parameters influencing the propagation are analyzed. The evolutions at the microstructure scale are compared with the macroscopic behavior of the specimen.

© 2021 The Authors. Published by Elsevier B.V.

This is an open access article under the CC BY-NC-ND license (<https://creativecommons.org/licenses/by-nc-nd/4.0>)

Peer-review under responsibility of the scientific committee of the Esiam organisers

Keywords: Additive Manufacturing ; 17-4PH ; SMAT ; Nanogauges gratings ; Crack propagation

* Corresponding author.

E-mail address: claire.gong@utt.fr

1. Introduction

The many advantages brought by additive manufacturing (AM) open new possibilities in creating complex parts and structures. It is possible to reduce the waste and to optimize the cost-effectiveness [Ngo et al. (2018)]. Thanks to these valuable assets, the popularity of AM leads to develop multiple process. Generally, polymeric and metallic materials are respectively used in material extrusion, such as fused filament fabrication (FFF) and powder bed-based processes. The AM of metals proposes itself multiple technics: laser beam melting (LBM), electron beam melting (EBM) and laser metal deposition (LMD) [Herzog et al. (2016)]. However, the main concern with AM is the anisotropy brought by the temperature gradient from the addition of successive layers [Carroll et al. (2015)]. One of the solution is to treat the material after the printing process.

The 17-4PH stainless steel is a material combining high-strength and good corrosion resistance. This precipitate hardening strength material is generally found in nuclear power plants [Bai et al. (2021)] or in marine environments [Murr et al. (2012)]. The treatment or functionalization of material surface can help to improve the mechanical properties like fracture initiation [Olugbade and Lu (2020)]. For example, Surface Mechanical Attrition Treatment (SMAT) gives a nanocrystallized surface and enhance hardness and tensile strength [Portella et al. (2020)].

The recent AM machine “Metal X” developed by Markforged Inc. combines the metal injection molding (MIM) with FFF [Metal AM (2017)]. The specimen obtained from this technic will be SMATed and characterized in order to evaluate the mechanical capacities of this process.

Moreover, it is challenging to characterize the crack initiation and thus studying the impact of SMAT on the material. The continuous progress made in electron beam lithography (EBL) in creating fine structures, capable of reaching the size of 10 nm [Tseng et al. (2003)], have opened new opportunities in material characterizations at local scale. Previous studies [Allais et al. (1994); Clair et al. (2011); Marae Djouda et al. (2017)] have exploited this progress by applying nanoparticles (NPs) periodic gratings on metallic substrates. During in-situ mechanical test under a scanning electron microscope (SEM), images are recorded, depicting the evolution of the NPs displacements in order to analyze microstructure feature.

In this article, a comparison between two types of metallic single edge notched tension (SENT) samples is presented: a SMATed sample and an as-fabricated (AF) sample, both under an in-situ tensile test in a SEM. Local crack initiation and propagation are observed and compared, exposing the influence of the post-treatment on the material properties.

2. Method

2.1. Specimen fabrication and preparation

Based on metal injection molding (MIM), the Atomic Diffusion Additive Manufacturing (ADAM) from Markforged combines the FFF technic with the washing and sintering process. Indeed, a polymeric binder is mixed with the metallic powder into a filament, which is then extruded with heat to print layer by layer the wanted part. To remove the majority of the binder, the as-printed piece is placed into a solvent. Then, the metallic part is sintered near its melting point, to eliminate any remain of the binder and to fuse the powder. Two SENT samples were printed with a Metal X System from Markforged, with a width of 300 μm and a layer of 50 μm for the post-sintered filament. The geometry of the specimens is detailed in Fig. 1(a) and the filament trajectory follows a 45°/-45° orientation, see Fig. 1(b). The notch geometry was conceived in accordance with the ASTM E1820 standard and the different lengths of the sample were designed following the NF EN ISO 6892-1 standard.

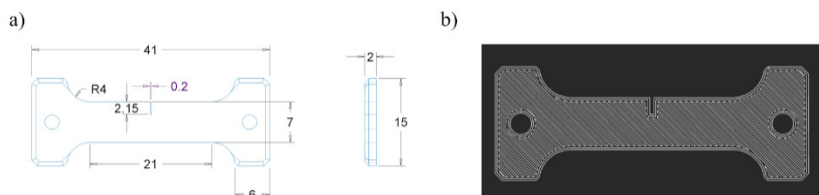


Fig. 1 a) Geometry of the sample printed, all dimensions are in mm. b) Trajectory of the nozzle, following a 45°/-45° orientation.

The samples were then polished thoroughly with a mechanical polishing until obtaining a mirror finish with a diamond paste of $1\mu\text{m}$, in order to remove the surface roughness, and thus to easily apply the nanogauges grating. The final thickness of the samples is equal to 1.2 mm in order to guaranty the fracture apparition for both samples during the test, since the maximum load applicable is 5000 N . One of the sample was SMATed after polishing and since this technic is based on plastic deformation induced by spherical shots, many parameters can have an influence on the surface outcome. The chosen parameters correspond to a SMAT High (30 minutes of treatment, 3 mm spherical shots, 20 kHz frequency, generator power at 27%) and are in accordance with the study of Portella et al. (2020). This choice ensures a satisfying modification of the surface structure but also the smoothest roughness among all the SMAT parameters studied. Portella et al. (2020) demonstrated a decrease of 94% of R_a with a SMAT High, from $11\mu\text{m}$ to $0.66\mu\text{m}$. In the present study, the average roughness R_a is $0.47\mu\text{m}$ for the SMATed sample.

2.2. Nanogauges gratings

The observation of crack initiation and propagation at the surface of the samples is quite challenging since the tip of the notch is 0.2 mm wide and the location of the crack is unknown until its appearance. Even if the method of the nanogauges gratings by EBL was used before, the area of deposition was however limited, in the range of a few micrometers.

The EBL process is composed by several steps [Corbier et al. (2005)]. After preparing the surface of the sample through polishing, a resin is deposited by spin coating and then exposed to a controlled electron beam, in order to have the pattern previously defined by the user. The exposed resin is removed, creating a mask for the gold layer to attach on the raw surface and on the resin. The last step, called lift-off, consists of dissolving the resin with a solvent, only leaving the gold particles on the substrate. Gold is a widespread material in the nanofabrication field for application at room temperature, as it is a conductive material and thus can offer a good image quality with a SEM [Khan et al. (2017)].

It is essential to obtain a large grating in order to cover the tip of the notch and to monitor the crack initiation. The deposition was realized by the Raith e-LiNE Electron Beam Lithography with a Polymethyl methacrylate (PMMA) resin and a new design of gratings was made to follow the crack. Indeed, a $400 \times 400\mu\text{m}^2$ was deposited on the surface, divided into sixteen $100 \times 100\mu\text{m}^2$ subgratings, separated by $1\mu\text{m}$ basic shapes particles (circles, triangles, squares and semi-circles). This innovative design is a response to a previous difficulty to locate correctly the area of observation when capturing images during the loading. Furthermore, this solution improves the tracking of the crack propagation through the test. In every subgratings, the NPs present a 200 nm diameter, a 50 nm height and a periodic distance of 400 nm between NPs centers. These parameters were chosen following the studies of Maraé Djouda et al. (2017), (2018) and (2019). It has the advantage to ensure a good spatial resolution and a good following of the NPs. Both samples show satisfying results regarding to the quality of the deposition, see Fig. 2 a) and b), demonstrating the capacity of EBL to apply a remarkably distinctive grating over an irregular surface.

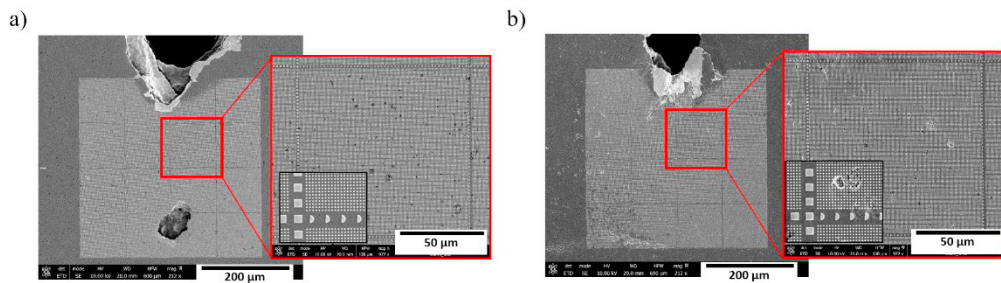


Fig. 2 a) Nanogauges gratings deposited on AF sample. b) Nanogauges gratings deposited on SMATed sample.

2.3. In-situ tensile test

After the deposition, the samples were put into a tensile test machine, inside a FEI Nova NanoSEM 450, see Fig. 3 a). Due to the delay for taking one picture with the SEM, the test has to be briefly stopped regularly, every 125 N ,

in order to capture alternatively the whole grating, then each $100 \times 100 \mu\text{m}^2$ subgratings in order to follow the crack evolution and its surrounding until the failure of the sample. Each image has a resolution of 4096×3775 pixels, ensuring a good quality of the nanogauges observation.

A number is assigned for each subgrating in order to follow their evolutions. The numbers are detailed in Fig. 3 b).

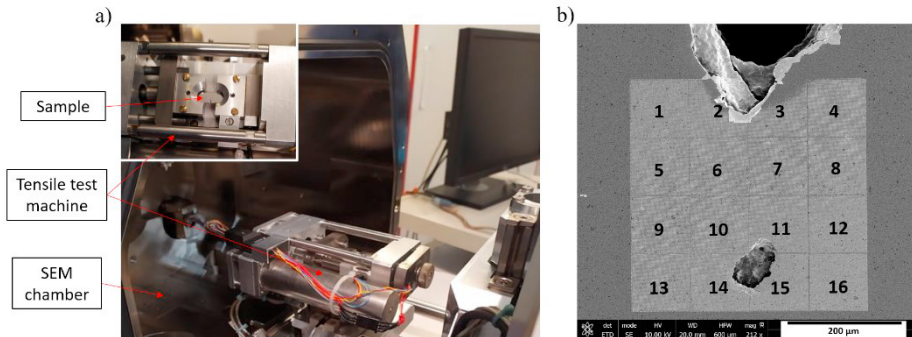


Fig. 3 a) Setup for the in-situ tensile test under the SEM. b) The assigned numbers for identifying each subgratings.

3. Results and discussion

3.1. Macroscopic stress-strain curves

The macroscopic stress-strain curves are presented in Fig. 4 a) for both samples. A magnification is available in Fig. 4 b) order to evidence the serration due the Portevin - Le Chatelier effect (PLC). Since the notch leads to a stress concentration in the middle of the samples, a stress concentration factor K_t is assumed to be equal to 3 for the calculation of the stress [Pilkey et al. (2020)].

The macroscopic stress-strain curves in Fig. 4 a) enable to evidence the effect of SMAT regarding to the final elongation. The post-treated sample achieves a fracture elongation of 2.04 % while the AF sample reaches 2.79 %. The strain hardening induced by the multiple impacts of the shots reinforces the surface and thus, the hardness of the sample [Portella et al, 2020]. However, the ultimate tensile strength (UTS) of the SMATed sample should be higher, as it was demonstrated in Portella et al. (2020) and Meng et al. (2018). The maximum stress applied for AF sample is 1919.8 MPa against 1838.8 MPa for the SMATed sample. It is worth noting that the macroscopic curves presented in this study are not from a continuous loading, as the test has to be paused in order to capture the SEM images, the macroscopic behavior of the sample can be influenced and the defects inherent to the fabrication process.

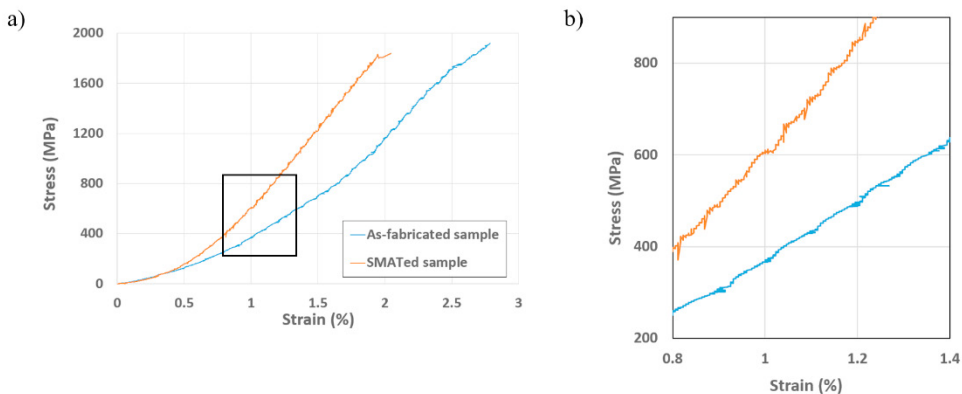


Fig. 4 a) Macroscopic stress-strain curves for both samples. b) Magnification of the area selected in a).

3.2. SEM images analysis for as-fabricated sample

The SEM images showed in Fig. 5 for AF sample are focusing on the subgrating number 3, as it depicts an insight of the crack initiation. Multiple cracks appeared on the image at 993 MPa but not all cracks are at the root of the notch. During the loading, the cracks n°2 and n°3 present a more important growth at 1470 MPa and 1602 MPa, as crack n°4 is slowly closed. At this moment, it can be difficult to predict which crack will be the cause of the sample failure. The presence of the porosity near the notch –framed in a red rectangle in Fig. 5–, displays a first crack inside at 1470 MPa and a second one at 1602 MPa. At 1638 MPa, a fifth crack appeared but the progression of crack n°2 leads to the failure of the sample. After 1752 MPa, it is evidenced that crack n°2 was greatly influenced by the presence of the nearest porosity. The same observation can be made for crack n°5 at 1752 MPa in Fig. 6, where four visible porosities were circled in red and judging by the crack trajectory, it appears that these defects served as a guide for crack up to the fracture.

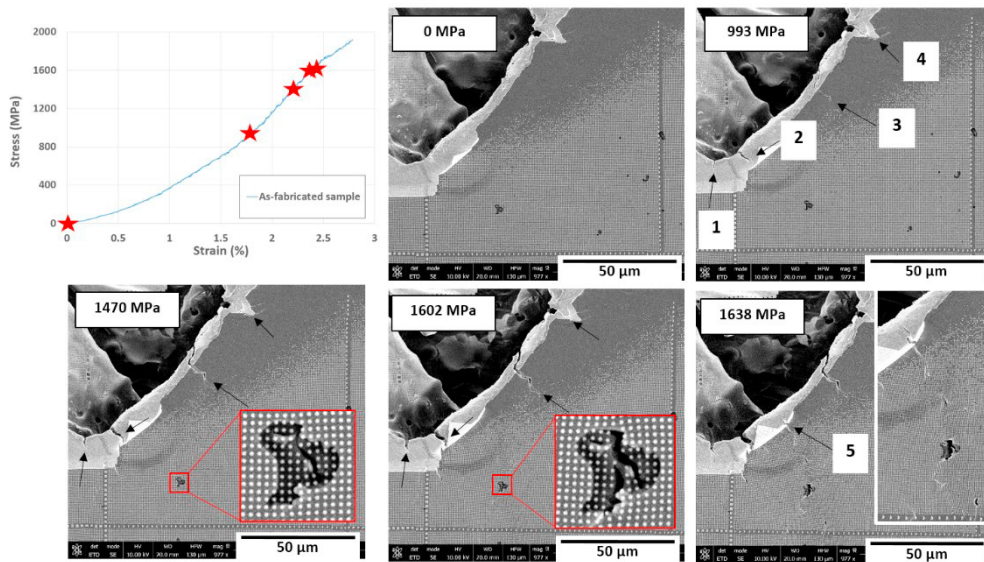


Fig. 5 Stress-strain curve and SEM images of the subgrating number 3 for the AF sample during the cracks evolutions.

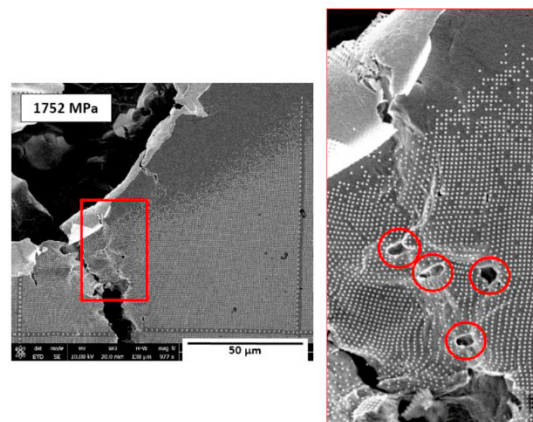


Fig. 6 SEM image of the subgrating number 3 at 1752 MPa and a magnification of the fifth crack following the multiple porosities.

3.3. SEM images analysis for SMATed sample

For SMATed sample in Fig. 7, the gradual crack initiation is inconspicuous, due to the topography after SMAT, leading to a more difficult examination of the crack evolutions. The plastic deformation, induced by the treatment, could have generated a material aggregation at the end of the notch. These accumulations areas will be called overlaps and can be seen in the red rectangles at 0 MPa in Fig. 7. As opposed to the previous observations with AF sample, the SMATed sample has only two observed cracks, located at material overlaps. Their different location is difficult to introduce in only one subgrating, the choice was made to follow the first line of subgratings, from n°1 to n°4.

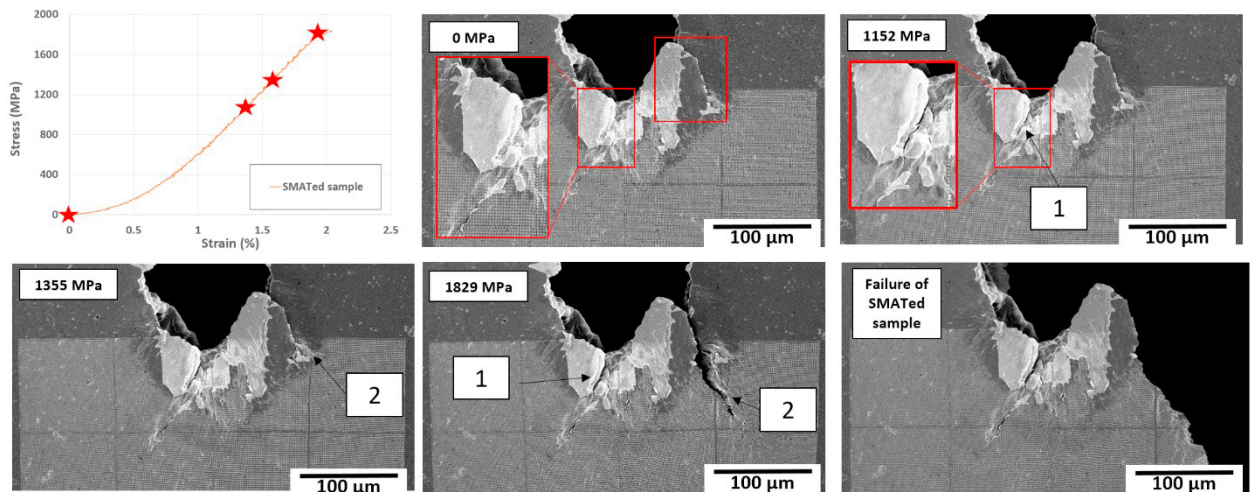


Fig. 7 SMATed sample stress-strain curve and SEM images of the cracks evolutions until failure.

The first crack appeared at 1152 MPa and at 1355 MPa for the second crack. The compressive residual stress induced by SMAT hinders the crack initiation as already observed in other studies [Coules et al. (2018)], delaying its apparition. The slow progression for both cracks is replaced by the crack n°2 sudden propagation at 1829 MPa. At the end of the loading, the crack n°2 is the cause of the failure of the sample, as shown in the last SEM image in Fig. 7 at the bottom right. The overlap may create stress concentration at their intersection, increasing the probability to create cracks at the surface. The behavior of the cracks showed during the loading leads to conclude that it may be possible to predict the location of the cracks by observing the overlap of the material near the notch. However, other tests should be conducted in order to completely validate this assumption.

4. Conclusion

In this study, an advanced method was used to characterize the crack initiation and propagation from a notch made by ADAM process.

The EBL technic allows the deposition of the nanogauges gratings, and the in-situ tensile test under a SEM allows the observation at a local scale. The roughness of the surface did not impact the quality of the deposition, demonstrating the robustness of the procedure.

The influence made by SMAT on final elongation and fracture evolution has been evidenced. The unique observations with SEM images bring more details and information on crack initiation and propagation, especially about their location and progression near the notch.

This method is a great solution for observing any specific areas for local characterization and in the future, predict possible crack initiation and optimize any parts or structures made by additive manufacturing.

References

- Allais L., Bornert M., Bretheau T., Caldemaison, D., 1994. "Experimental characterization of the local strain field in a heterogeneous elastoplastic material". *Acta metallurgica et Materialia* 3865–3880.
- Bai, Bing, Rong Hu, Changyi Zhang, Jing Xue, and Wen Yang. "Effect of Precipitates on Hardening of 17-4PH Martensitic Stainless Steel Serviced at 300 °C in Nuclear Power Plant". *Annals of Nuclear Energy* 154, p. 108123. <https://doi.org/10.1016/j.anucene.2020.108123>.
- Carroll, Beth E., Todd A. Palmer, and Allison M. Beese. "Anisotropic Tensile Behavior of Ti–6Al–4V Components Fabricated with Directed Energy Deposition Additive Manufacturing". *Acta Materialia* 87, p.309-320. <https://doi.org/10.1016/j.actamat.2014.12.054>.
- Clair, A., M. Foucault, O. Calonne, Y. Lacroute, L. Markey, M. Salazar, V. Vignal, and E. Finot. "Strain Mapping near a Triple Junction in Strained Ni-Based Alloy Using EBSD and Biaxial Nanogaugess". *Acta Materialia* 59, no 8, p. 3116-3123. <https://doi.org/10.1016/j.actamat.2011.01.051>.
- Corbierre, Muriel K., Jean Beerens, and R. Bruce Lennox. "Gold Nanoparticles Generated by Electron Beam Lithography of Gold(I)–Thiolate Thin Films". *Chemistry of Materials* 17, no 23: 5774-79. <https://doi.org/10.1021/cm051085b>.
- Coules, H. E., G. C. M. Horne, K. Abburi Venkata, and T. Pirling. "The Effects of Residual Stress on Elastic-Plastic Fracture Propagation and Stability". *Materials & Design* 143: 131-40. <https://doi.org/10.1016/j.matdes.2018.01.064>.
- Herzog, Dirk, Vanessa Seyda, Eric Wycisk, and Claus Emmelmann. "Additive Manufacturing of Metals". *Acta Materialia* 117: 371-92. <https://doi.org/10.1016/j.actamat.2016.07.019>.
- Khan, Ibrahim, Khalid Saeed, and Idrees Khan. "Nanoparticles: Properties, Applications and Toxicities". *Arabian Journal of Chemistry* 12, no 7: 908-31. <https://doi.org/10.1016/j.arabjc.2017.05.011>.
- Marae Djouda, Joseph, Yazid Madi, Fabrice Gaslain, Jeremie Beal, Jerome Crepin, Guillaume Montay, Lea Le Joncour, Naman Recho, Benoit Panicaud, and Thomas Maurer. "Investigation of Nanoscale Strains at the Austenitic Stainless Steel 316L Surface: Coupling between Nanogauges Gratings and EBSD Technique during in Situ Tensile Test". *Materials Science and Engineering: A* 740-741. 315-35. <https://doi.org/10.1016/j.msea.2018.10.059>.
- Marae Djouda, Joseph, Guillaume Montay, Benoit Panicaud, Jeremie Beal, Yazid Madi, and Thomas Maurer. "Nanogaugess Gratings for Strain Determination at Nanoscale". *Mechanics of Materials* 114, p. 268-78. <https://doi.org/10.1016/j.mechmat.2017.08.014>.
- Marae Djouda, Joseph, Benoit Panicaud, Fabrice Gaslain, Jeremie Beal, Yazid Madi, Guillaume Montay, Lea Le Joncour, and al. "Local Microstructural Characterization of an Aged UR45N Rolled Steel: Application of the Nanogauges Grating Coupled EBSD Technique". *Materials Science and Engineering: A* 759: 537-51. <https://doi.org/10.1016/j.msea.2019.05.059>.
- Meng, Xiangchen, Bei Liu, Lan Luo, Yan Ding, Xi-Xin Rao, Bin Hu, Yong Liu, and Jian Lu. "The Portevin-Le Chatelier Effect of Gradient Nanostructured 5182 Aluminum Alloy by Surface Mechanical Attrition Treatment". *Journal of Materials Science & Technology* 34, no 12: 2307-15. <https://doi.org/10.1016/j.jmst.2018.06.002>.
- Murr, Lawrence E., Edwin Martinez, Jennifer Hernandez, Shane Collins, Krista N. Amato, Sara M. Gaytan, and Patrick W. Shindo. "Microstructures and Properties of 17-4 PH Stainless Steel Fabricated by Selective Laser Melting". *Journal of Materials Research and Technology* 1, no 3: 167-77. [https://doi.org/10.1016/S2238-7854\(12\)70029-7](https://doi.org/10.1016/S2238-7854(12)70029-7).
- Ngo, Tuan D., Alireza Kashani, Gabriele Imbalzano, Kate T. Q. Nguyen, and David Hui. "Additive Manufacturing (3D Printing): A Review of Materials, Methods, Applications and Challenges". *Composites Part B: Engineering* 143: 172-96. <https://doi.org/10.1016/j.compositesb.2018.02.012>.
- Olugbade, Temitope Olumide, and Jian Lu. "Literature Review on the Mechanical Properties of Materials after Surface Mechanical Attrition Treatment (SMAT)". *Nano Materials Science, Special Issue: Nanostructured metals and alloys*, 2, no 1: 3-31. <https://doi.org/10.1016/j.nanoms.2020.04.002>.
- Pilkey, Walter D., Deborah F. Pilkey, and Zhuming Bi. "Peterson's stress concentration factors". John Wiley & Sons, 2020, p. 105.
- Portella, Q., M. Chemkhii, and D. Retraint. "Influence of Surface Mechanical Attrition Treatment (SMAT) Post-Treatment on Microstructural, Mechanical and Tensile Behaviour of Additive Manufactured AISI 316L". *Materials Characterization* 167, p. 110463. <https://doi.org/10.1016/j.matchar.2020.110463>.
- "THE MAGAZINE FOR THE METAL ADDITIVE MANUFACTURING INDUSTRY 'METAL AM,'" Inovar Communications Ltd, vol. 3, no. 2, 2017.
- Tseng, Ampere A., Kuan Chen, Chii D. Chen, and Kung J. Ma. "Electron Beam Lithography in Nanoscale Fabrication: Recent Development". *IEEE Transactions on Electronics Packaging Manufacturing*, 2003, 141-49.